FERMILAB-CONF-08-487-CD

Testing the Standard Model with $W\gamma$ and $Z\gamma$ at the Tevatron

Adam L. Lyon (for the CDF and D0 collaborations)
Fermi National Accelerator Laboratory, Batavia, IL 60510, USA

Results on analyses involving $W\gamma$ and $Z\gamma$ production from the CDF and D0 experiments at the Fermilab Tevatron Collider at $\sqrt{s} = 1.96$ TeV are presented here. Using 1-2 fb^{-1} of data, cross sections, anomalous coupling limits, and the $W\gamma$ Radiation Amplitude Zero are reviewed.

1. INTRODUCTION

Boson self-interactions are a consequence of $SU(2)_L \times U(1)_Y$ gauge symmetry. Certain self-interactions such as $WW\gamma$ are required by the standard model (SM), while others such as $ZZ\gamma$ and $Z\gamma\gamma$ are forbidden. If these trilinear-gauge couplings are not as the SM predicts, then new physics may lead to striking deviations in the kinematics of the process compared to the SM prediction, such as enhancement of the photon energy spectrum at large E_T^γ.

The $W\gamma$ process offers another window on new physics. Gauge theory predicts that any four particle tree amplitude involving one or more gauge bosons may be factorized into a part depending on charge alone and a second part depending on spin and polarization. At a particular point in phase space, the charge part will cause the amplitude to vanish. For $W\gamma$, this effect leads to a zero[1] (the Radiation Amplitude Zero, RAZ) in the angular distribution of the photon in the CM frame of the incoming quarks. But in hadron collisions determination of this frame is difficult because the direction of the ν that decayed from the W is unknown. Therefore instead, the charge-signed rapidity difference[2] defined to be $Q_\ell \times \Delta y$ (Q_ℓ is the charge of the ℓ decayed from the W and Δy is the $\ell - \gamma$ rapidity difference) is used. At the Tevatron, the psuedorapidity difference ($\Delta\eta$) is an accurate replacement for Δy. The RAZ then appears as a dip in this distribution at $Q_\ell \times \Delta\eta \approx -1/3$. Non-SM trilinear-gauge couplings act to wash out the dip as does final state radiation.

The key to the analyses described here is excellent photon identification. Photons appear similar to electrons in detectors, but photons do not have an associated track. Both CDF and D0 utilize preshowers to enhance discrimination of photons against jets. D0 uses calorimeter layers as well as the preshower measurement to point back to the vertex of the photon to further reject jets. CDF also removes photons generated by electron bremsstrahlung with tracks in the silicon detector. Photon efficiency is mainly determined by Monte Carlo studies, but for low energies it is possible to verify the simulations with low energy final state radiation $Z\gamma$ events.

2. $Z\gamma \rightarrow \ell\ell\gamma$

In the SM at tree level, $Z\gamma$ is produced by initial state radiation (ISR) and final state radiation (FSR) diagrams shown in Fig. 1. The SM forbids the s-channel diagram involving the trilinear gauge couplings. Cross sections are measured with $ee\gamma$ and $\mu\mu\gamma$ events. The D0 analysis[3] is based on 1.1 fb^{-1} of data while the CDF analysis[4] is based on 1.1 fb^{-1} of data in the electron channel and 2 fb^{-1} in the muon channel. Both analyses require central photons with $E_T^\gamma > 7$ GeV and a minimum ΔR between a lepton and the photon of 0.7. The minimum di-lepton invariant mass is 30 GeV/c^2 and 40 GeV/c^2 for D0 and CDF respectively.

The cross section measurements are shown in Table I. The E_T^γ spectra are shown in Fig. 2. No deviation from the SM prediction is observed.

Limits are placed on on anomalous $ZZ\gamma$ and $Z\gamma\gamma$ couplings. $ZV\gamma$ couplings (where V is either Z or γ) are parameterized by CP violating parameters (h_1^V, h_2^V) and CP conserving parameters (h_3^V, h_4^V). All vanish in the SM. In the case of non-SM physics, these couplings may rise with CM energy and violate unitarity. To avoid that problem, it is typical to transform these couplings with a form factor $h \rightarrow h/(1 + \hat{s}/\Lambda^2)^n$. Both experiments choose $\Lambda = 1.2$ TeV. 95% CL limits on the real parts of the CP conserving couplings are shown in Table II. For the Tevatron,

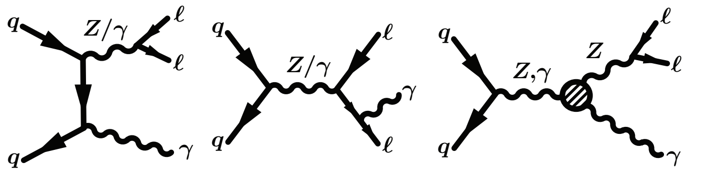

Figure 1: Diagrams for $Z\gamma$ production: ISR, FSR and the forbidden s-channel involving the trilinear gauge coupling.

Table I: Cross section results for $Z\gamma$ analyses.

Value	Observed	SM Expectation
CDF	E_T^γ >7 GeV, ΔR >0.7, $M_{\ell\ell}$ >40 GeV/c^2	
ISR+FSR	778 events (390 $ee\gamma$ + 388 $\mu\mu\gamma$)	771 ± 41
ISR+FSR	σ(pb) = 4.6 ± 0.2(stat) ± 0.3(sys) ± 0.3(lum)	4.5 ± 0.4
ISR	σ(pb) = 1.2 ± 0.1(stat) ± 0.2(sys) ± 0.1(lum)	1.2 ± 0.1
FSR	σ(pb) = 3.4 ± 0.2(stat) ± 0.2(sys) ± 0.2(lum)	3.3 ± 0.3
D0	E_T^γ >7 GeV, ΔR >0.7, $M_{\ell\ell}$ >30 GeV/c^2	
ISR+FSR	968 events (453 $ee\gamma$ + 515 $\mu\mu\gamma$)	920.4 ± 53.4
ISR+FSR	σ(pb) = 5.0 ± 0.3(stat+sys) ± 0.3(lum)	4.74 ± 0.22

lmits on the CP violating couplings are nearly identical to the corresponding CP conserving couplings. The combined LEP2 results[5] are shown as well.

3. $W\gamma \to \ell\nu\gamma$

$W\gamma$ production proceeds through three diagrams plus FSR (the s-channel diagram with the $WW\gamma$ coupling is required by the SM) as shown in Fig. 3. A CDF analysis[6] measures the $W\gamma$ production cross section with 1 fb^{-1} of data with $W\gamma \to \ell\nu\gamma$ events where ℓ is an e or μ. The analysis requires central photons with $E_T^\gamma > 7$ GeV, missing $E_T > 25$ (20) GeV for the e (μ) analysis, $\Delta R_{\ell\gamma} > 0.7$, $\ell\nu$ transverse mass between 30 and 120 GeV/c^2, and central electrons and muons with $E_T^e > 25$ GeV and $E_T^\mu > 20$ GeV. The combined cross section is measured to be $\sigma(W\gamma) \times \mathrm{BR}(W \to \ell\nu) = 18.03 \pm 0.65_{\mathrm{stat}} \pm 2.55_{\mathrm{sys}} \pm 1.05_{\mathrm{lum}}$ pb. This value compares well with the SM prediction of 19.3 ± 1.4 pb. The E_T^γ spectrum is shown in Fig. 4.

The corresponding D0 analysis[7] is optimized to examine the RAZ discussed above and examined 700 pb^{-1} of

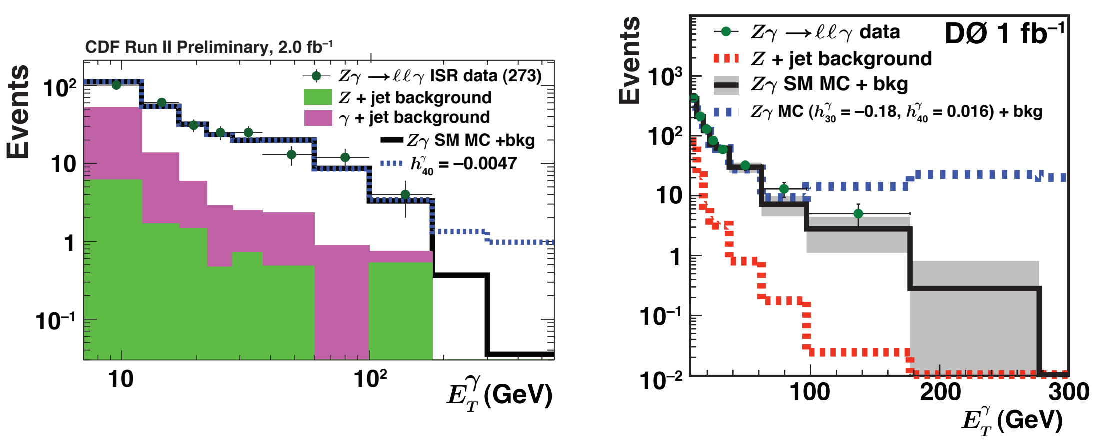

Figure 2: Photon E_T spectra in $Z\gamma$ production for the CDF and D0 analyses respectively.

Table II: 95% CL limits on $ZZ\gamma$ and $Z\gamma\gamma$ couplings.

	CDF (1.1 fb^{-1} e, 2.0 fb^{-1} μ)	DØ 1.1 fb^{-1}	LEP2 2003
h_3^γ	$[-0.084, 0.084]$	$[-0.085, 0.084]$	$[-0.049, -0.008]$
h_4^γ	$[-0.0047, 0.0047]$	$[-0.0053, 0.0054]$	$[-0.002, -0.034]$
h_3^Z	$[-0.083, 0.083]$	$[-0.083, 0.082]$	$[-0.20, 0.07]$
h_4^Z	$[-0.0047, 0.0047]$	$[-0.0053, 0.0054]$	$[-0.05, 0.12]$

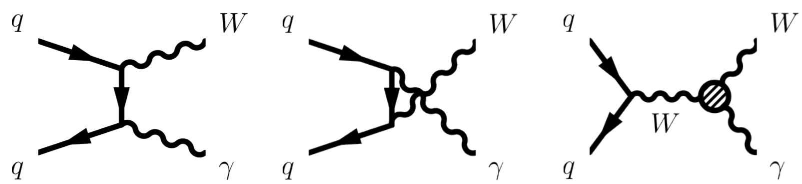

Figure 3: ISR and s-channel diagrams for $W\gamma$ production. The FSR diagram is not shown.

data. Here, forward photons are crucual for measuring $Q_\ell \times \Delta\eta$. Requirements are central and forward photons with $E_T^\gamma > 9$ GeV, missing $E_T > 25\,(20)$ GeV for the electron and muon analysis respectively and $\Delta R_{\ell\gamma} 0.7$. The electron analysis additionally requires a central or forward electron with $E_T > 25$ GeV, $e\nu$ transverse mass > 50 GeV$/c^2$, and three body transverse mass M_{T3} (e, γ, and missing E_T) > 120 GeV/c^2. The muon analysis requires a muons within $|\eta| < 1.6$ with $p_T > 20$ GeV$/c$ and $M_{T3} > 110$ GeV$/c^2$. The M_{T3} cuts are optimized to reject FSR events as they will obscure the dip. The background subtracted signal yields are $130 \pm 14 \pm 3.4$ for $e\nu\gamma$ events and $57 \pm 8.8 \pm 1.8$ for the $\mu\nu\gamma$ events (uncertainties are statistical and systematic respectively). These results compare well to the SM predictions of 120 ± 12 and 77 ± 9.4 for $e\nu\gamma$ and $\mu\nu\gamma$ respectively. The measured E_T^γ spectrum is displayed in Fig. 4. No deviation from the SM is observed. Using the photon E_T spectrum, 95% CL limits on anomalous $WW\gamma$ couplings are determined to be $0.49 < \kappa_\gamma < 1.51$, $-0.12 < \lambda_\gamma < 0.13$ where in the SM coupling parameters $\kappa_\gamma = 1$ and $\lambda_\gamma = 0$ (for this analysis form factor $\Lambda = 2$ TeV). These limits are the best at a hadron collider and are a direct examination of the $WW\gamma$ vertex.

The background subtracted data are used to construct the $Q_\ell \times \Delta\eta$ distribution as shown on the left in Fig 5. Depicted on the right in Fig 5 is a study to determine the significance of the dip that is apparent in the $Q_\ell \times \Delta\eta$ distribution. Two bins are chosen, one that for the SM covers the dip region and an equally sized bin to its left that samples the preceding peak (see the inset in the figure). The ratio of events in the dip bin to the small maximum bin

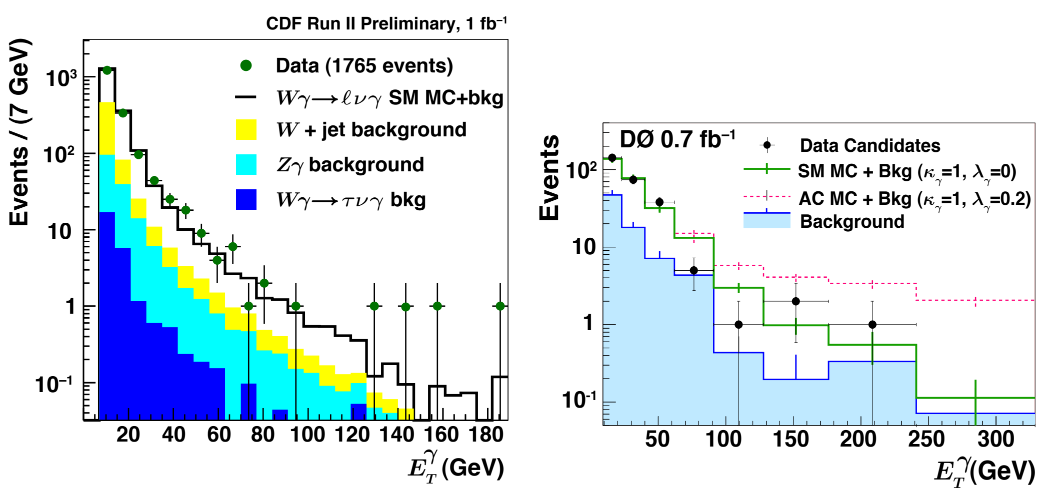

Figure 4: Photon E_T spectra for the CDF and D0 $W\gamma$ analyses respectively.

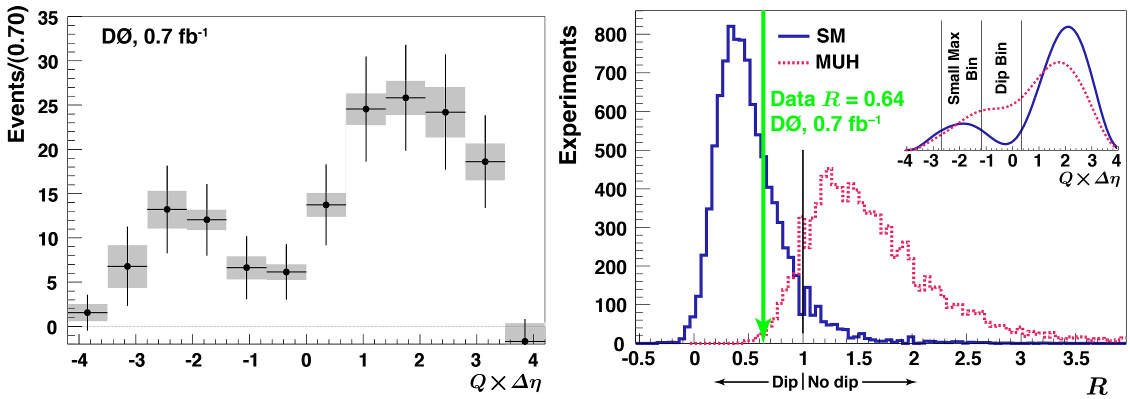

Figure 5: $Q_\ell \times \Delta\eta$ distribution (left) and its analysis (right).

(R) is measured. If $R < 1$ then a dip is observed. A value of $R = 0.64$ is observed in the data. A minimal unimodal hypothesis (MUH) is generated with anomalous couplings – this model is on the verge of not having a dip. 10,000 pseudo-experiments (SM and MUH) are performed to determine the significance of the R value. In the ensemble tests, 28% of SM experiments had a higher value of R, indicating that the measurement is consistent with the SM. Only 45 MUH experiments out of 10,000 had an R value below the data. The conclusion is that the probability that a MUH hypothesis could fluctuate to the data R value or lower is $45/10,000; p = (4.5 \pm 0.7) \times 10^{-3}$ corresponding to a Gaussian 2.6σ. D0 thus makes the first measurement of the $Q_\ell \times \Delta\eta$ distribution and it is indicative of the RAZ of the Standard Model.

4. CONCLUSIONS

Diboson physics is extremely important for testing the Standard Model. $W\gamma$ and $Z\gamma$ production show no hints of a deviation from the SM. Therefore, limits were set on anomalous couplings. The Radiation Amplitude Zero in the $W\gamma$ system is also measured via the charge-signed rapidity distribution for the first time.

Acknowledgments

The author wishes to thank the staffs at Fermilab and collaborating institutions as well as the respective funding agencies for CDF and D0.

References

1 R. W. Brown, D. Sahdev, and K. O. Mikaelian, Phys. Rev. D **20**, 1164 (1979); K. O. Mikaelian, M. A. Samuel, and D. Sahdev, Phys. Rev. Lett. **43**, 746 (1979); C. J. Goebel, F. Halzen, and J. P. Leveille, Phys. Rev. D **23**, 2682 (1981); S. J. Brodsky and R. W. Brown, Phys. Rev. Lett. **49**, 966 (1982).
2 U. Baur, S. Errede, and G. Landsberg, Phys. Rev. D **50**, 1917 (1994).
3 V.M. Abazov *et al.* (D0 Collaboration), Phys. Lett. B **653**, 378 (2007).
4 Preliminary analysis. See `http://www-cdf.fnal.gov/physics/ewk/2008/Zgamma/`
5 LEP2 TGC Working Group, LEPEWWG/TGC/2003-01, `http://lepewwg.web.cern.ch/LEPEWWG/lepww/tgc/summer03/gc_main2003.ps`
6 Preliminary analysis. See `http://www-cdf.fnal.gov/physics/ewk/2007/wgzg/`
7 V.M. Abazov *et al.* (D0 Collaboration), Phys. Rev. Lett., **100**, 131801 (2008).